Two-magnon Raman scattering in a Mott-Hubbard antiferromagnet

Saurabh Basu and Avinash Singh
Department of Physics, Indian Institute of Technology, Kanpur 208016, India
(Received 28 June 1995; revised manuscript received 29 February 1996)

A perturbation-theoretic diagrammatic scheme is developed for systematically studying the two-magnon Raman scattering in a Mott-Hubbard antiferromagnet. The fermionic structure of the magnon interaction vertex is obtained at order-$1/\mathcal{N}$ level in an inverse-degeneracy expansion, and the relevant two-magnon propagator is obtained by incorporating magnon interactions at a ladder-sum level. Evaluation of the magnon interaction vertex in the large-U limit yields a nearest-neighbor instantaneous interaction with interaction energy $-J$. Application of this approach to the intermediate-U regime, which is of relevance for cuprate antiferromagnets, is also discussed. Incorporating the zero-temperature magnon damping, which is estimated in terms of quantum spin fluctuations, the two-magnon Raman scattering intensity is evaluated and compared with experiments on La_2CuO_4. [S0163-1829(96)05430-6]

I. INTRODUCTION

Two-magnon Raman scattering has been used as a probe to study low-energy excitations in magnetic solids, particularly the short-wavelength modes. Extensive studies have been carried out in antiferromagnets such as $RbMnF_3$, MnF_2, and K_2NiF_4,[1–5] and a good theoretical understanding exists for these systems with spin $S \geqslant 1$, within the interacting-magnon theory for the quantum Heisenberg antiferromagnet (QHAF).[6] Recently there has been renewed interest since studies in La_2CuO_4 (a $S=1/2$ system) have indicated evidence of substantial quantum spin fluctuations,[7–9] and the observed two-magnon Raman scattering linewidth is much too broad to be explained within the classical theory.[4] Moreover, scattering intensities are observed in geometries which, in the classical approximation, should yield no scattering. Interest in two-magnon Raman scattering continues also because upon doping with holes, the two-magnon peak broadens out and relaxes into the Raman continuum. In $YBa_2Cu_3O_{6+x}$, for example, the intensity of the two-magnon feature decreases rapidly with increasing x, and virtually disappears at $x=0.5$.[10]

While theoretically two-magnon Raman scattering has been studied extensively within the QHAF, there have been so far only limited attempts to systematically study this within the Mott-Hubbard model. Recently a strong-coupling expansion in powers of t/U, the hopping term, has been carried out, and the Fleury-Loudon Hamiltonian has been obtained at the second order level.[11] In this treatment, the hopping term is extended to include the gauge term $\exp[(ie/\hbar c)\int_i^j \mathbf{A}\cdot\mathbf{dl}]$ arising from the external transverse electro magnetic field, and the transition matrix elements which determine the Raman scattering are obtained within a strong-coupling expansion. However, it appears that so far no systematic, formally weak-coupling expansion has been carried out which can continuously interpolate between the small-U and large-U limits.

Significantly, in the small- and intermediate-U regimes of the Mott-Hubbard antiferromagnet, when the interaction term U is less than or comparable to the free-electron bandwidth W, the one-magnon density of states (DOS) exhibits a peak structure which broadens and shifts to lower energies with decreasing U.[12,13] In contrast, in the large-U limit, the one-magnon DOS diverges at the upper band edge due to zone-boundary magnons at energy DJ, where $J=4t^2/U$ is the exchange energy and D the dimensionality. This peak structure resembles a broadening due to a magnon interaction, and must be incorporated in any realistic theory of two-magnon Raman scattering when applied to the small- and intermediate-U regimes. Since it is believed that La_2CuO_4 does actually fall in the intermediate-U regime, a formally weak-coupling expansion scheme has a potential application as well.

In this paper we describe a perturbation-theoretic diagrammatic scheme for systematically obtaining the two-magnon Raman scattering in the Mott-Hubbard antiferromagnet. Since within the Hubbard model itself there is no formal expansion parameter, we make use of the generalized Hubbard model with $\mathcal{N}$ orbitals per site,[14] and develop a systematic expansion in powers of $1/\mathcal{N}$. This perturbation-theoretic scheme, which preserves the spin rotational symmetry, and hence the Goldstone mode, order by order in the perturbation theory, has been used earlier to systematically obtain quantum corrections to sublattice magnetization, spin-wave energy, perpendicular susceptibility, and ground-state energy of a Hubbard antiferromagnet.[14] When this formally weak-coupling perturbative approach is carried to the large-U (strong-coupling) limit, which is analytically the simplest, one recovers identical results as obtained within the $1/S$ expansion for the spin-S quantum Heisenberg model. We shall see that this holds for the two-magnon Raman scattering effect as well.

In spin-pair excitations by light, the two magnons are created on nearest-neighbor (NN) sites, and therefore strong interaction effects between magnons are important in a quantitative analysis. Considering a two-dimensional $S=1/2$ system for concreteness, two spins flipped involve an excitation energy $4J$ when far apart but only energy $3J$ when on NN sites. This suggests that the interaction energy between magnons at the lowest-order level is $-J$ when on NN sites, which shifts the peak in the two-magnon Raman scattering intensity to energy $\sim 3J$. Indeed, we find within our perturbation-theoretic approach that to the lowest order in $1/\mathcal{N}$, the interaction energy between magnons on NN sites is

precisely $-J$ in the large-U limit.

We first consider, in the next section, the large-U limit wherein the magnon propagator and magnon interaction are considered at the lowest-order level in an expansion in powers of t^2/U^2. In this limit only the nearest-neighbor Heisenberg antiferromagnetic interaction $J=4t^2/U$ is present in the equivalent spin model. In Sec. III we consider an extension to the intermediate-U regime by incorporating higher-order terms in the magnon propagator and interactions. Finally in Sec. IV we make a simple estimate for zero-temperature magnon damping and evaluate the Raman scattering intensity in the B_{1g} symmetry and compare with the observed Raman scattering in La_2CuO_4.

II. LARGE-U LIMIT

The scattering of light in magnetic solids can be described by the Fleury-Loudon effective Hamiltonian which represents the interaction of spin pairs with photon pairs:

$$H_R=A\sum_{\mathbf{r},\boldsymbol{\delta}}(\mathbf{E}_{\rm inc}\cdot\boldsymbol{\delta})(\mathbf{E}_{\rm sc}\cdot\boldsymbol{\delta})\boldsymbol{S}(\boldsymbol{r})\cdot\boldsymbol{S}(r+\boldsymbol{\delta}). \tag{1}$$

Here $\mathbf{E}_{\rm inc}$, and $\mathbf{E}_{\rm sc}$ are the incident and the scattered electric field vectors, and $\boldsymbol{\delta}$ is a unit vector connecting nearest-neighboring sites of opposite sublattices. The sum over $\boldsymbol{r}$ ensures that the spin-pair excitation has zero total wave vector as required by momentum conservation since the photons involved have essentially zero wave vector. To calculate the two-magnon spectrum, we need to extract parts of the spin operators which combine to create a pair of magnons. We focus therefore on the transverse part of the spin-pair operator $P_{\boldsymbol{\delta}}\equiv\Sigma_{\boldsymbol{r}}\boldsymbol{S}(\boldsymbol{r})\cdot\boldsymbol{S}(\boldsymbol{r}+\boldsymbol{\delta})$. Since the two-magnon Raman scattering intensity is related to the correlation function of the spin-pair operator $P_{\boldsymbol{\delta}}$, which can be obtained as the imaginary part of the corresponding propagator, we consider the following time-ordered two-magnon Green's function:

$$G_{\boldsymbol{\delta},\boldsymbol{\delta}'}(\Omega)=-i\int dt e^{i\Omega(t-t')}\times\left\langle\psi_G\middle|T\left[\sum_{\boldsymbol{r}}S^-(\boldsymbol{r},t)S^+(\boldsymbol{r}+\boldsymbol{\delta},t)\times\sum_{\boldsymbol{r}'}S^+(\boldsymbol{r}',t')S^-(\boldsymbol{r}'+\boldsymbol{\delta}',t')\right]\middle|\psi_G\right\rangle. \tag{2}$$

As mentioned earlier, in this paper we develop a systematic perturbation expansion for this two-magnon propagator within the Hubbard model. We show the fermionic structure of the magnon-interaction vertex to $O(1/\mathcal{N})$, and evaluate the resulting two-magnon propagator in the large-U limit in order to make contact with the known results within the Heisenberg model formalism. Extension to higher orders in $(1/\mathcal{N})$ and to the intermediate-U regime can then be carried out. We first consider the noninteracting limit of the two-magnon propagator $G^0_{\boldsymbol{\delta},\boldsymbol{\delta}'}(\Omega)$, decompose it into the irreducible representations of the lattice, and then develop the perturbative expansion in powers of the magnon interaction. In the noninteracting limit we have a magnon pair propagating from NN sites $\boldsymbol{r},\boldsymbol{r}+\boldsymbol{\delta}$ to $\boldsymbol{r}',\boldsymbol{r}'+\boldsymbol{\delta}'$; and in terms of the magnon propagators χ^{-+} and χ^{+-}, we obtain for the two-magnon propagator in the noninteracting limit

$$G^0_{\boldsymbol{\delta},\boldsymbol{\delta}'}(\Omega)=i\int dt e^{i\Omega(t-t')}\sum_{\mathbf{r},\mathbf{r}'}\chi^{-+}(\boldsymbol{r},t;\boldsymbol{r}',t')\times\chi^{+-}(\boldsymbol{r}+\delta,t;\boldsymbol{r}'+\boldsymbol{\delta}',t'). \tag{3}$$

The one-magnon propagator χ^{-+} has been studied within the Hubbard model in the large-U limit,[15] and also in the intermediate-U regime.[12] In the antiferromagnet translational invariance holds only within each sublattice, and therefore Fourier transformation within a two sublattice basis yields the magnon propagator $\chi^{-+}(\boldsymbol{r},t;\boldsymbol{r}',t')$ in terms of a 2×2 matrix $[\chi^{-+}(Q,\Omega)]$. At the random phase approximation (RPA) level the one-magnon propagator has the following form in the strong-coupling limit of a Hubbard antiferromagnet on a hypercubical lattice in D dimensions:

$$\chi^{-+}(Q,\Omega)=-\frac{1}{2}\left(\frac{DJ}{\Omega_Q}\right)\begin{bmatrix}1-\dfrac{\Omega}{DJ} & -\gamma_Q\\ -\gamma_Q & 1+\dfrac{\Omega}{DJ}\end{bmatrix}\times\left(\frac{1}{\Omega-\Omega_Q}-\frac{1}{\Omega+\Omega_Q}\right), \tag{4}$$

where $\Omega_Q=DJ\sqrt{1-\gamma_Q^2}$ is the magnon energy and $\gamma_Q=\Sigma_{\mu=1}^{D}\cos Q_\mu/D$. Now since $\boldsymbol{\delta},\boldsymbol{\delta}'$ are vectors joining nearest neighbors, if $\boldsymbol{r}$ and $\boldsymbol{r}'$ belong to sublattices μ and ν, respectively $(\mu,\nu=A/B)$, then $r+\boldsymbol{\delta}$ and $\boldsymbol{r}'+\boldsymbol{\delta}'$ belong to opposite sublattices $\bar{\mu}$ and $\bar{\nu}$, respectively, and therefore we obtain

$$G^0_{\boldsymbol{\delta},\boldsymbol{\delta}'}(\Omega)=i\int\frac{d\Omega_1}{2\pi}\sum_Q\sum_{\mu\nu}[\chi^{-+}(Q,\Omega_1)]_{\mu\nu}\times[\chi^{+-}(-Q,\Omega-\Omega_1)]_{\bar{\mu}\bar{\nu}}e^{i\mathbf{Q}\cdot(\boldsymbol{\delta}-\boldsymbol{\delta}')}. \tag{5}$$

It is convenient to (i) decompose $G^0_{\boldsymbol{\delta},\boldsymbol{\delta}'}(\Omega)$ in terms of the irreducible representations $\phi_n(Q)$ of the lattice and (ii) consider G^0 in a 2×2 matrix form within the two-sublattice basis. This greatly simplifies the summation of the perturbative series in powers of magnon interaction, as we will see later. For the nth irreducible representation, we obtain

$$[G^0_n(\Omega)]_{\mu\nu}=i\int\frac{d\Omega_1}{2\pi}\sum_Q\phi_n^2(Q)[\chi^{-+}(Q,\Omega_1)]_{\mu\nu}\times[\chi^{+-}(-Q,\Omega-\Omega_1)]_{\bar{\mu}\bar{\nu}}. \tag{6}$$

Finite-temperature evaluation of $[G^0_n(\Omega)]_{\mu\nu}$ can now be carried out in the standard way. Replacing the frequency Ω by the bosonic Matsubara frequency $i\Omega_m$ and the frequency integral over Ω_1 by a contour integral, and taking the contour around each singularity in the clockwise direction, we obtain

$$[G_n^0(i\Omega_m)]_{\mu\nu}=i\oint\frac{d\Omega_1}{2\pi}\sum_Q\ \phi_n^2(Q)[\chi^{-+}(Q,\Omega_1)]_{\mu\nu}\times[\chi^{+-}(-Q,i\Omega_m-\Omega_1)]_{\mu\nu}\frac{1}{e^{\beta\Omega_1}-1}. \tag{7}$$

Adding the residues from the four poles, taking $e^{\beta i\Omega_m}=1$, and finally replacing $i\Omega_m$ by Ω, yields the following matrix elements of $[G_n^0(\Omega)]$:

$$[G_n^0(\Omega)]_{AA}=\sum_Q\ \phi_n^2(Q)\left(\frac{DJ}{\Omega_Q}\right)^2\left[1+\left(\frac{\Omega_Q}{DJ}\right)^2-\left(\frac{\Omega}{DJ}\right)\right]\times\frac{\Omega_Q}{\Omega^2-4\Omega_Q^2}\coth\left(\frac{\beta\Omega_Q}{2}\right),$$

$$[G_n^0(\Omega)]_{BB}=\sum_Q\ \phi_n^2(Q)\left(\frac{DJ}{\Omega_Q}\right)^2\left[1+\left(\frac{\Omega_Q}{DJ}\right)^2+\left(\frac{\Omega}{DJ}\right)\right]\times\frac{\Omega_Q}{\Omega^2-4\Omega_Q^2}\coth\left(\frac{\beta\Omega_Q}{2}\right),$$

$$[G_n^0(\Omega)]_{AB}=\sum_Q\ \phi_n^2(Q)\left(\frac{DJ}{\Omega_Q}\right)^2[\gamma_Q^2]\frac{\Omega_Q}{\Omega^2-4\Omega_Q^2}\coth\left(\frac{\beta\Omega_Q}{2}\right)=[G_n^0(\Omega)]_{BA}. \tag{8}$$

Adding these four matrix elements allows for all possibilities regarding positions of $\mathbf{r}$ and $\mathbf{r}'$, and imaginary part of the sum yields the noninteracting limit of the two-magnon Raman scattering intensity,

$$R_n^0(\Omega)=\sum_Q\ \phi_n^2(Q)\left(\frac{DJ}{\Omega_Q}\right)^2\delta(\Omega-2\Omega_Q)\times\coth\left(\frac{\beta\Omega_Q}{2}\right)\frac{1}{1-e^{-\beta\Omega}}, \tag{9}$$

which is essentially the joint magnon density of states near the upper end of the magnon spectrum where $\Omega_Q\sim DJ$, and peaks at $\Omega=2DJ$. Finite-temperature corrections are negligible at temperatures $k_BT\ll J$.

We now turn to the magnon interaction vertex within the Hubbard model, and obtain its fermionic structure at the lowest-order level $O(1/\mathcal{N})$. The magnon interaction vertex is evaluated in the large-U limit, wherein we only retain terms of order t^2/U^2 and neglect terms of order t^4/U^4 and smaller. $t^4/U^4\sim J^2/U^2$ is a measure of the next-nearest-neighbor (NNN) spin-spin interaction within the equivalent extended-range Heisenberg model, and $O(J^2/U^2)$ terms will be included in the intermediate-U regime. The fermionic structure of the magnon interaction vertex, when the interacting magnons are on opposite sublattices, is shown in Fig. 1. There are eight diagrams which contribute at the $O(1/\mathcal{N})$ level to the magnon interaction vertex. These diagrams essentially describe various $\uparrow$-spin and $\downarrow$-spin particle-hole processes involving the nearest-neighboring sites. The $+/-$ signs in these diagrams refers to the advanced/retarded nature of the one-particle Green's function, corresponding to states in the upper/lower Hubbard bands. The fermionic propagator signs indicated in the diagrams are not exhaustive of all possibilities, but correspond to choices which yield leading-order contribution at the t^2/U^2 level. The contributions of diagrams shown in Fig. 1(a)–(h) are given in Table 1, and a detailed evaluation of one of the diagrams is given in the Appendix. Up to order t^2/U^2 the net contribution of all diagrams of $O(1/\mathcal{N})$ to the magnon interaction vertex is given by

TABLE I. Contributions to the magnon-interaction vertex of diagrams shown in Figs. 1(a)–1(h), for various signs of the pair of fermion propagators which are off diagonal in sublattice basis. The fermion-propagator signs refer to the advanced/retarded nature of the fermionic propagators.

Diagrams	Fermion-propagator signs	Contribution
Figs. 1(a), 1(b)	$(++),(--)$	$(JD/2)\gamma_{Q-Q'}$
Figs. 1(a), 1(b)	$(+-),(-+)$	$-2(JD/2)\gamma_{Q-Q'}$
Figs. 1(c), 1(d)	$(--)$	$(JD/2)\gamma_{Q-Q'}$
Figs. 1(c), 1(d)	$(+-),(-+)$	$-(JD/2)\gamma_{Q-Q'}$
Figs. 1(e), 1(f)	$(++)$	$(JD/2)\gamma_{Q-Q'}$
Figs. 1(e), 1(f)	$(+-),(-+)$	$-(JD/2)\gamma_{Q-Q'}$
Figs. 1(g), 1(h)	$(+-),(-+)$	$(JD/2)\gamma_{Q-Q'}$

$$V_{\rm int}(\mathbf{Q}-\mathbf{Q}',\Omega_1-\Omega_2)=-2DJ\gamma_{\mathbf{Q}-\mathbf{Q}'}, \tag{10}$$

implying nearest-neighbor instantaneous interaction energy $-J$ between magnons. In the magnon interaction vertex the entering and exiting magnon lines involve the same sublattice, and in fact the same site in large-U limit, so that in real space we can write $V_{\rm int}(\boldsymbol{r},\boldsymbol{r}',\boldsymbol{r}+\boldsymbol{\delta},\boldsymbol{r}'+\boldsymbol{\delta}')=V_{\rm int}(\boldsymbol{r},\boldsymbol{r},\boldsymbol{r}+\boldsymbol{\delta},\boldsymbol{r}+\boldsymbol{\delta})=-J$. Therefore in the two-sublattice basis the magnon interaction vertex is diagonal: $[V_{\rm int}(\mathbf{Q}-\mathbf{Q}')]_{\mu\nu}=-zJ\gamma_{\mathbf{Q}-\mathbf{Q}'}\delta_{\mu\nu}$ where $z=2D$ is the coordination number of the lattice. We also make use of the irreducible representations $\phi_n(\mathbf{Q})$ of the lattice to decouple the momentum dependence of the interaction vertex as

$$V_{\rm int}(\mathbf{Q}-\mathbf{Q}')=-zJ\gamma_{\mathbf{Q}-\mathbf{Q}'}=-J\sum_n\ \phi_n(\mathbf{Q})\phi_n(\mathbf{Q}'). \tag{11}$$

Here the irreducible representations $\phi_n(Q)$ are normalized so that $\Sigma_Q\phi_n^2(Q)=1$ for all n. This decoupling permits a straightforward summation of the perturbation series for the two-magnon propagator $G_n(\Omega)$ involving repeated magnon interactions in a ladder sum. The orthogonality of the irreducible representations $\phi_n(Q)$ leads to the following result in the two sublattice basis:

$$[G_n(\Omega)]=\frac{[G_n^0(\Omega)]}{1+J[G_n^0(\Omega)]}. \tag{12}$$

Again we need to add the four matrix elements of $[G_n(\Omega)]$ so as to allow for all possibilities regarding positions of $\boldsymbol{r}$ and $\boldsymbol{r}'$. If we use $A(\Omega)$, $B(\Omega)$, and $C(\Omega)$ to denote the matrix elements $[G_n^0(\Omega)]_{AA}$, $[G_n^0(\Omega)]_{BB}$, and $[G_n^0(\Omega)]_{AB/BA}$, respectively, which are given in Eq. (8), then the sum of matrix elements of $[G_n(\Omega)]$ is obtained as below. The imaginary part then yields $R_n(\Omega)$, the two-magnon Raman scattering intensity for a Hubbard antiferromagnet, in the strong-coupling limit, at the ladder-sum level:

$$\sum_{\mu\nu}[G_n(\Omega)]_{\mu\nu}=\frac{(A+B+2C)+2J(AB-C^2)}{(1+JA)(1+JB)-J^2C^2}. \quad (13)$$

Within the Heisenberg formalism, using a perturbative approach in which the magnon-magnon interaction was taken into account in a ladder approximation, this result was obtained earlier by Solyom.[16] In this work four vertex functions were introduced corresponding to the four possibilities arising from the incoming and outgoing magnon lines belonging to the two sublattices. These vertex functions were obtained, within the ladder approximation, in the form of coupled equations, which were then solved and added to yield $\Sigma_{\mu\nu}[G_n(\Omega)]_{\mu\nu}$. On the other hand, by expressing the two-magnon propagator in the two-sublattice basis as 2×2 matrix, we are able to perform the ladder sum in a very straightforward manner, and summing the matrix elements *at the end* yields the same result. Of course our starting point is the Hubbard model, and we have treated the Hubbard interaction term perturbatively within a formally weak-coupling expan-

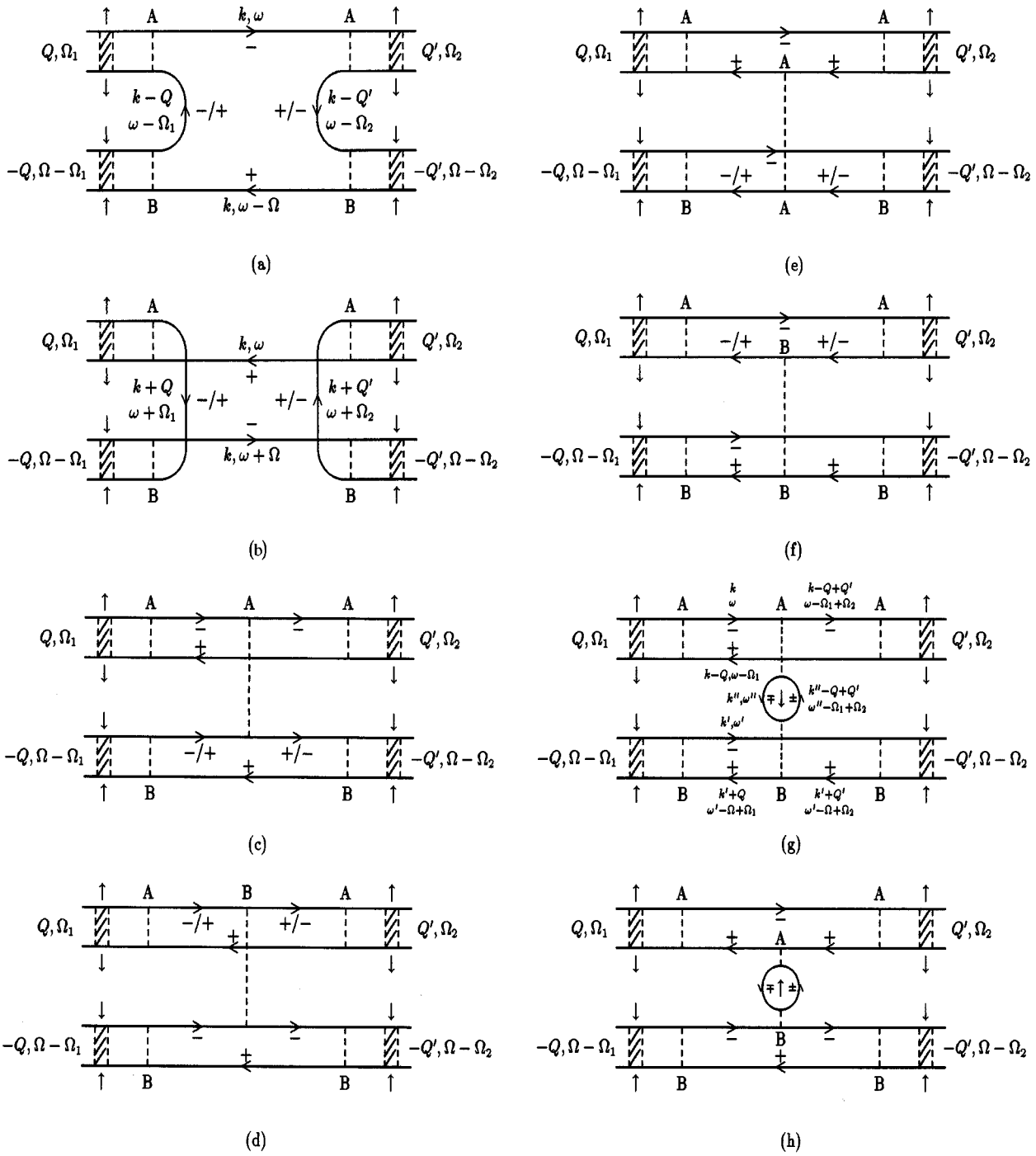

FIG. 1. Fermion structure of the diagrams contributing to the magnon-interaction vertex at the order $1/\mathcal{N}$ level and in the strong-coupling limit. The interacting magnons are on A- and B-sublattice sites. The interaction vertices lie within the four dashed lines representing the Hubbard interaction. The hatched areas represent the magnon propagators.

sion scheme, and carrying this expansion to the strong-coupling limit we have recovered the Solyom result. Our approach can therefore be extended to the intermediate-U and small-U regimes as well in principle.

Finally we consider the Ising limit of the expression for the two-magnon propagator given in Eq. (13), in order to clearly see the role of the nearest-neighbor magnon interaction. In the Ising limit when the spins can only be flipped completely, the spin-wave (spin-flip) energy is DJ, $\gamma_Q=0$ and therefore $A=C=0$ and

$$B=\sum_Q \phi_n^2(Q)\left(\frac{1}{\Omega-2DJ}-\frac{1}{\Omega+2DJ}\right)$$
$$=\left(\frac{1}{\Omega-2DJ}-\frac{1}{\Omega+2DJ}\right).$$

In this limit $\Sigma_{\mu\nu}[G_n(\Omega)]_{\mu\nu}$ reduces to the following equation which shows the pole at $\Omega=2DJ-J$ corresponding to the two-magnon spin-flip excitations created on nearest-neighbor sites:

$$\sum_{\mu\nu}[G_n(\Omega)]_{\mu\nu}|_{\text{Ising}}=\frac{1}{\Omega-2DJ+J}. \tag{14}$$

Several extensions of this analysis of two-magnon Raman scattering in the Hubbard model, carried out here in the large-U limit, are possible, some of which are discussed below. Higher-order corrections in the inverse-degeneracy expansion in powers of $1/\mathcal{N}$ may be included in the magnon interaction vertex. Magnon damping which may be systematically incorporated in the theory in this manner is of particular interest because, after all, one-magnon states are not exact eigenstates of the antiferromagnet, and hence damping of magnon modes is expected, particularly of the short-wavelength, high-energy modes. Also the one-magnon lines themselves may be renormalized to include the magnon interaction effects. At the $O(1/\mathcal{N})$ level the spin-wave energies are modified by the momentum-independent multiplicative factor Z_c ($=1.16$ in $2D$, e.g.), and the spin-wave amplitude is reduced by the same factor as the sublattice magnetization relative to the Hartree-Fock (HF) value. Also of interest is the extension to the intermediate-U regime which is discussed below.

III. INTERMEDIATE-U REGIME

In the intermediate-U regime the Hubbard model maps to an extended-range Heisenberg model and the NNN spin couplings of $O(t^4/U^3)$ can be obtained within the RPA analysis.[12] Alternatively the magnon-interaction vertices of Fig. 1 can be evaluated up to the next order $O(t^4/U^4)$. Thus with the one-magnon propagator $\chi^{-+}(\Omega)$ and the magnon interaction vertex both evaluated up to $O(t^4/U^4)$, one can systematically study the two-magnon Raman scattering in the intermediate-U regime. As mentioned earlier this regime is of interest because the modification of spin-wave spectrum results in a significantly different form of the magnon density of states. Instead of the divergence at energy $2J$ in the DOS due to zone-boundary magnons, one instead gets a peak structure with a progressively increasing broadening as U/t decreases. This peak structure resembles the effect of magnon damping and therefore any quantitative treatment of two-magnon Raman scattering in the intermediate-U regime must take this intrinsic broadening into account. Here we consider a simple extension to the intermediate-U regime.

There are essentially two modifications that are required in our earlier analysis. Both the NN magnon-interaction energy and the spin-wave propagator acquire an order t^2/U^2 correction. Using the results of Ref. 12 where spin-wave properties were obtained via a systematic expansion in powers of t^2/U^2, we obtain after a zero-temperature evaluation of the two-magnon propagator the following matrix elements of $[G_n^0(\Omega)]$, the zeroth-order two-magnon propagator, given in Eq. (8):

$$A(\Omega)=\sum_Q m^2\phi_n^2(Q)\left(\frac{2J}{\Omega_Q}\right)^2$$
$$\times\left[a^2-\left(\frac{\Omega_Q}{2J}\right)^2-a\frac{\Omega}{2J}+\frac{1}{2}\left(\frac{\Omega}{2J}\right)^2\right]\frac{\Omega_Q}{\Omega^2-4\Omega_Q^2},$$

$$B(\Omega)=\sum_Q m^2\phi_n^2(Q)\left(\frac{2J}{\Omega_Q}\right)^2$$
$$\times\left[a^2-\left(\frac{\Omega_Q}{2J}\right)^2+a\frac{\Omega}{2J}+\frac{1}{2}\left(\frac{\Omega}{2J}\right)^2\right]\frac{\Omega_Q}{\Omega^2-4\Omega_Q^2},$$

$$C(\Omega)=\sum_Q m^2\phi_n^2(Q)\left(\frac{2J}{\Omega_Q}\right)^2[b^2\gamma_Q^2]\frac{\Omega_Q}{\Omega^2-4\Omega_Q^2}, \tag{15}$$

where $m=1-2t^2/\Delta^2$ is the magnetization at the HF level, $2\Delta=mU$ is the Hubbard gap, and up to order t^2/Δ^2 we have, in the intermediate-U regime,

$$\Omega_Q=2J\left[(1-\gamma_Q^2)-\frac{t^2}{\Delta^2}(6+3\cos Q_x\cos Q_y-9\gamma_Q^2)\right]^{1/2},$$

$$a=1-\frac{t^2}{\Delta^2}\left(3+\frac{3}{2}\cos Q_x\cos Q_y+\gamma_Q^2\right), b=1-\frac{t^2}{\Delta^2}\left(\frac{11}{2}\right). \tag{16}$$

A simple estimate for the NN magnon-interaction energy is now made as follows. We have seen that in the large-U limit, this interaction energy is nothing but the NN spin-interaction energy. Since this result is consistent with the simple bond counting argument, we expect this to hold in the intermediate-U regime as well. Therefore we take the NN magnon-interaction energy to be simply the modified NN spin-interaction energy. An elementary quantitative analysis which relies on a comparison of spin-wave energy forms for the intermediate-U Hubbard model (evaluated up to order t^2/Δ^2) and the NNN Heisenberg model is given in Appendix B and yields, for the NN spin-interaction energy, $J_{\text{NN}}=J(1-\frac{9}{2}t^2/\Delta^2)$.

The two-magnon Raman scattering intensity for the two-dimensional system is now evaluated in the intermediate-U regime from $G_n(\Omega)=G_n^0(\Omega)/[1+J_{\text{NN}}G_n^0(\Omega)]$ and is shown in Fig. 2 for the case $\Delta/t=3.5$ which corresponds to $U\sim W$ for the two-dimensional case. We have taken the symmetry factor $\phi_n(\mathbf{Q})=(\cos Q_x-\cos Q_y)$, appropriate to the B_{1g} symmetry. Comparing with the large-U limit result, it is

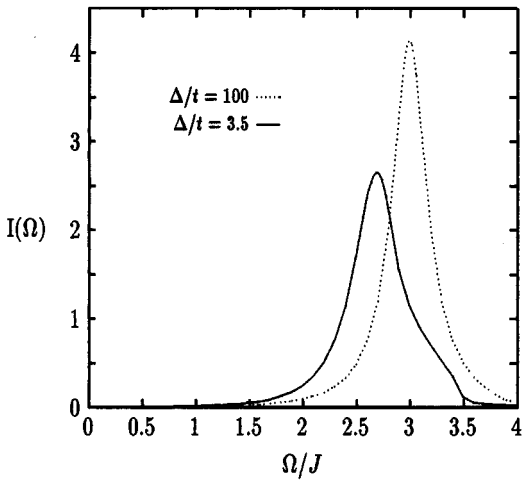

FIG. 2. Calculated two-magnon Raman scattering intensity in the B_{1g} symmetry in the large-U limit (dotted line) and the intermediate-U limit (solid line).

clear that while there is a 25% increase in the linewidth in going to the intermediate U, this increase is not sufficient to account for the zero-temperature linewidth observed in La_2CuO_4. Therefore, while this contribution must be taken into account in any quantitative analysis, the large broadening seen in La_2CuO_4 must find an explanation elsewhere. In the flowing we consider an important source of broadening which is particularly relevant for La_2CuO_4 which is a low-spin and low-dimensional system.

IV. ZERO-TEMPERATURE MAGNON DAMPING

It is well established now that quantum spin fluctuations play an important role in La_2CuO_4 and other cuprate antiferromagnets which are spin-1/2 and almost two-dimensional systems. There is a substantial reduction in the zero-temperature sublattice magnetization relative to the HF (Néel) value. Thus while long-range AF order is maintained in the two-dimensional (2D) antiferromagnet, there is substantial amount of spin disorder. A consequence of this fluctuation-induced disorder is that spin-wave states are not exact eigenstates of the antiferromagnetic ground state, so that spin-wave or magnon damping must necessarily be present. And since two-magnon Raman scattering is related to the imaginary part of the two-magnon propagator, magnon damping should play an important role in the observed broadening.

While finite-temperature magnon damping in the Heisenberg antiferromagnet has been studied in detail,[17–19] zero-temperature magnon damping is not easy to obtain in the antiferromagnetic insulator. The second-order magnon interaction process does not yield any damping at zero temperature owing to a phase-space restriction. This process involves a magnon decaying into three magnons which subsequently reunite. From simple energy-momentum conservation considerations it is seen that for lightlike linear dispersion this process has a vanishingly small phase space. This argument in fact holds for any convex energy-momentum dispersion, as for magnons.

We discuss below a simple estimate for zero-temperature magnon damping which is based on the following disorder analogy. Because of the substantial transverse spin fluctuations present in the $S=1/2$, $D=2$ antiferromagnetic insulator, magnons propagating in the system will see a fairly disordered magnetic lattice in which the spins, while maintaining overall AF long-range order, are slowly fluctuating in space and time. These fluctuations are slow on the time scale of $(2J)^{-1}$ and therefore zone-boundary, high-energy magnons of energy $2J$, which are of interest, will see an essentially static disorder. This disorder-analogy picture suggests that magnon damping will be proportional to the magnon density of states, which results in a qualitatively correct picture — substantial damping for zone-boundary magnons and very small damping for low-energy, long-wavelength magnons. Since we are interested only in the zone-boundary magnons, in view of the divergent magnon density of states at the upper edge at $2J$, a self-consistent evaluation of damping is therefore essential. We obtain the self-consistent magnon damping for zone-boundary magnons with energy $\Omega \sim 2J$:

$$\Gamma = \gamma \, \mathrm{Im} \sum_Q [\chi^{-+}(Q,\Omega)] = \gamma \sum_Q \frac{2J}{\Omega_Q} \frac{\Gamma}{(\Omega-\Omega_Q)^2+\Gamma^2}, \tag{17}$$

where γ is an effective disorder strength which measures the degree of spin disorder due to quantum transverse fluctuations, which we now proceed to estimate. An appropriate measure of transverse spin fluctuations is the equal-time correlation function $\langle S^- S^+ \rangle$, and therefore the simplest estimate for the scattering vertex is $J\langle S^- S^+ \rangle$. And since the disorder strength γ represents two scattering processes, we obtain $\gamma \sim J^2 \langle S^- S^+ \rangle^2$. Now for the $D=2$, $S=1/2$ antiferromagnet, we know $\langle S^- S^+ \rangle = \Sigma_Q (1/\sqrt{1-\gamma_Q^2}) - 1)/2 \approx 0.2$, which is precisely the quantum-fluctuation reduction in $\langle S_z \rangle$ or the sublattice magnetization.

Substituting this value of γ, the effective disorder strength, we self-consistently solve from Eq. (17) the effective one-magnon damping for zone-boundary magnons, and obtain $\Gamma/J = 0.15$. Thus even for zone-boundary magnons the resulting damping is small — only about 7% of the energy. We now incorporate this magnon damping arising from quantum spin fluctuations into the two-magnon Raman scattering evaluation from Eq. (13) in the large-U limit. This is done by simply adding the imaginary part $2i\Gamma$ to the two-magnon energy $2\Omega_Q$ in the energy denominators in Eq. (8). We take the symmetry factor $\phi_n(\mathbf{Q}) = (\cos Q_x - \cos Q_y)$, appropriate to the B_{1g} symmetry, for comparison with Raman scattering observations on La_2CuO_4. The result of this evaluation, together with the Raman intensity observed in La_2CuO_4 taken from Ref. 8, is shown in Fig. 3. We adjust the energy scales so that the observed Raman peak at around 3200 cm^{-1} occurs at $3J$ where our calculated Raman scattering intensity peaks. As we have shown earlier, there will be additional broadening if the evaluation is done in the intermediate-U regime, appropriate to the cuprates. It is clear that while the linewidth compares reasonably well with the observed full width at half maximum (FWHM) of about 1200 cm^{-1}, there is a marked asymmetry in the observed Raman line, and also a significantly larger scattering persisting at energies above $4J$. It has been suggested that four-magnon excitations are responsible for these features.

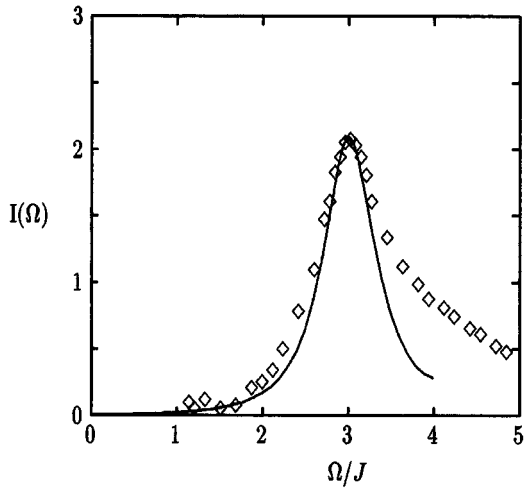

FIG. 3. Calculated two-magnon Raman scattering intensity in the B_{1g} symmetry with a magnon damping of $\Gamma/J=0.15$, and few points from the observed Raman scattering in La_2CuO_4 (taken from Ref. 8).

There have been several recent studies of two-magnon Raman scattering in antiferromagnetic insulators where various additional aspects have been investigated and proposed as being significant besides the quantum-spin-fluctuation effects. These include magnetostriction-induced exchange disorder introduced by lattice vibrations,[20] magnon damping caused by magnon-phonon interaction,[21,22] and resonant Raman scattering in which the incident photon energy is comparable to the Hubbard gap.[23] It thus appears that the actual physics involved in the two-magnon Raman scattering experiments on antiferromagnetic insulators like cuprates may be quite rich in detail.

APPENDIX A

In this appendix we discuss evaluation of diagrams shown in Figs. 1(a)–1(h) representing magnon interaction vertices relevant for the two-magnon propagator. The vertices are shown for interaction between magnons on opposite sublattices A and B. The evaluation is performed in the strong-coupling limit, in which case the interaction is actually effective only on nearest-neighbor sites. As mentioned earlier the interaction vertices represent spin-$\uparrow$, spin-$\downarrow$ particle-hole processes in which energy momentum is exchanged by the interacting magnons. All diagrams shown are of order $1/\mathcal{N}$ in an inverse-degeneracy expansion.

We first briefly review the single-particle Green's functions in the AF state in the strong-coupling limit.[15]. In terms of the quasiparticle amplitudes $a^s_\sigma(\mathbf{k})$ and $b^s_\sigma(\mathbf{k})$ on the two sublattices, the single-particle Green's functions are given by

$$G^s_\sigma(\mathbf{k},\omega)=\begin{bmatrix}(a^s_\sigma)^2 & a^s_\sigma b^s_\sigma\\ a^s_\sigma b^s_\sigma & (b^s_\sigma)^2\end{bmatrix}\frac{1}{\omega-E^s_{\mathbf{k}}+is\eta}, \tag{A1}$$

where $\sigma=\uparrow/\downarrow$, and $s=+/-$ referring to states in the upper/lower Hubbard band. Here the quasiparticle energy $E^\pm_{\mathbf{k}}=\pm\sqrt{\Delta^2+\epsilon^2_{\mathbf{k}}}$, where $2\Delta=mU$ is the Hubbard gap, and $\epsilon_{\mathbf{k}}=-2t\Sigma^D_{\mu=1}\cos k_\mu$ is the free-particle energy. From spin-sublattice symmetry, $(a^-_\uparrow)^2=(b^+_\downarrow)^2$ and $(a^+_\uparrow)^2=(b^-_\downarrow)^2$. In the strong-coupling limit, retaining terms only up to order t^2/U^2, we have $a^-_\uparrow(\mathbf{k})^2=b^+_\downarrow(\mathbf{k})^2=1-\epsilon^2_{\mathbf{k}}/U^2$ and $a^+_\uparrow(\mathbf{k})=b^-_\downarrow(\mathbf{k})=\epsilon_{\mathbf{k}}/U$.

Now in each diagram there are precisely two fermionic lines connecting an A-sublattice site to a B-sublattice site, and therefore off diagonal in the two-sublattice basis. This pair of lines already contributes a factor t^2/U^2, and therefore we need to retain only the leading-order contributions from all other terms in each diagram. As a representative example, we discuss the evaluation of the diagram shown in Fig. 1(g), where the fermion lines constituting the loop are off diagonal in the sublattice basis. The amplitudes of all other Green's functions are taken to be 1 and poles at energy $E^\pm_{\mathbf{k}}=\pm U/2$, in order to obtain the leading-order contribution. Contributions of all diagrams shown in Figs. 1(a)–1(h) are given in Table I. To the magnon-interaction vertex the contribution of diagram shown in Fig. 1(g) is given by

$$\begin{aligned}
&V_{\rm int}(\mathbf{Q}-\mathbf{Q}',\Omega_1-\Omega_2)|_{(g)}\\
&=i(iU)^6\int\frac{d\omega}{2\pi}\sum_{\mathbf{k}}\,G^-_\uparrow(\mathbf{k},\omega)_{AA}G^-_\uparrow(\mathbf{k}-\mathbf{Q}+\mathbf{Q}',\omega-\Omega_1+\Omega_2)_{AA}G^+_\downarrow(\mathbf{k}-\mathbf{Q},\omega-\Omega_1)_{AA}\\
&\times\int\frac{d\omega'}{2\pi}\sum_{\mathbf{k}'}\,G^-_\downarrow(\mathbf{k}',\omega')_{BB}G^+_\uparrow(\mathbf{k}'+\mathbf{Q},\omega'-\Omega+\Omega_1)_{BB}G^+_\uparrow(\mathbf{k}'+\mathbf{Q}',\omega'-\Omega+\Omega_2)_{BB}\\
&\times(-1)\int\frac{d\omega''}{2\pi}\sum_{\mathbf{k}''}\,G^\mp_\downarrow(\mathbf{k}'',\omega'')_{AB}G^\pm_\downarrow(\mathbf{k}''-\mathbf{Q}+\mathbf{Q}',\omega''-\Omega_1+\Omega_2)_{BA}\\
&=(iU)^6\int\frac{d\omega}{2\pi i}\sum_{\mathbf{k}}\left(\frac{1}{\omega-(-U/2)-i\eta}\right)^2\left(\frac{1}{\omega-U/2+i\eta}\right)\int\frac{d\omega'}{2\pi i}\sum_{\mathbf{k}'}\left(\frac{1}{\omega-(-U/2)-i\eta}\right)\left(\frac{1}{\omega-U/2+i\eta}\right)^2\\
&\times(-1)\int\frac{d\omega''}{2\pi i}\sum_{\mathbf{k}''}\left(\frac{\epsilon_{\mathbf{k}''}/U}{\omega''-(\mp U/2)\mp i\eta}\right)\left(\frac{\epsilon_{\mathbf{k}''-\mathbf{Q}+\mathbf{Q}'}/U}{\omega''-(\pm U/2)\pm i\eta}\right)\\
&=(iU)^6\left(\frac{-1}{U^2}\right)\left(\frac{1}{U^2}\right)(-1)\left(\frac{-1}{U^3}\right)\sum_{\mathbf{k}''}\,\epsilon_{\mathbf{k}''}\epsilon_{\mathbf{k}''-\mathbf{Q}+\mathbf{Q}'}=\frac{4t^2}{U}\frac{D}{2}\gamma_{\mathbf{Q}-\mathbf{Q}'}=(JD/2)\gamma_{\mathbf{Q}-\mathbf{Q}'}.
\end{aligned}\tag{A2}$$

APPENDIX B

We discuss below an estimation of the NN spin-interaction energy in the intermediate-U regime. The idea is to compare the spin-wave energy expressions obtained from (i) the spin-1/2 Heisenberg model with NNN spin interaction and (ii) the intermediate-U Hubbard model, both for the two-dimensional, square-lattice case. If J and J' refer to the NN and NNN Heisenberg antiferromagnetic spin interactions, respectively, then for the spin-wave energy we have

$$\Omega_Q \approx 2J[(1-\gamma_Q^2)-(2J'/J)(1-\gamma_Q')]^{1/2}, \tag{B1}$$

where $\gamma_{\mathbf{Q}}' \equiv \cos Q_x \cos Q_y$, and terms of order $(J'/J)^2$ have been neglected. We compare this expression now with the result for the Hubbard model obtained at the RPA level by an expansion[12] in powers of t^2/Δ^2, where $2\Delta = mU$ is the Hubbard gap:

$$\Omega_Q = 2(4t^2/U)[(1-\gamma_Q^2)-(t^2/\Delta^2)(6+3\gamma_Q'-9\gamma_Q^2)]^{1/2}, \tag{B2}$$

which, after separating the γ_Q and γ_Q' pieces, can be rewritten as

$$\Omega_Q \approx 2(4t^2/U)(1-9t^2/\Delta^2)^{1/2} \times[(1-\gamma_Q^2)+(3t^2/\Delta^2)(1-\gamma_Q')]^{1/2}. \tag{B3}$$

Now comparing these two spin-wave energy expressions, we obtain for the NN spin coupling

$$J \approx \frac{4t^2}{U}\left(1-\frac{9}{2}\frac{t^2}{\Delta^2}\right) \tag{B4}$$

and a *ferromagnetic* NNN spin coupling

$$\frac{J'}{J} = -\frac{3}{2}\frac{t^2}{\Delta^2}. \tag{B5}$$

[1] R. J. Elliott, M. F. Thorpe, G. F. Imbusch, R. Loudon, and J. B. Parkinson, Phys. Rev. Lett. **21**, 147 (1968).
[2] P. A. Fleury, Phys. Rev. Lett. **21**, 151 (1968).
[3] M. F. Thorpe, J. Appl. Phys. **41**, 892 (1970).
[4] J. B. Parkinson, J. Phys. C **2**, 2012 (1969).
[5] P. A. Fleury and H. J. Guggenheim, Phys. Rev. Lett. **24**, 1346 (1970).
[6] R. J. Elliott and M. F. Thorpe, J. Phys. C **2**, 1630 (1969).
[7] K. Lyons, P. A. Fleury, J. P. Remeika, A. S. Cooper, and T. J. Negran, Phys. Rev. B **37**, 2353 (1988).
[8] R. R. P. Singh, P. A. Fleury, K. B. Lyons, and P. E. Sulewski, Phys. Rev. Lett. **62**, 2736 (1989).
[9] P. E. Sulewski, P. A. Fleury, K. B. Lyons, S-W. Cheong, and Z. Fisk, Phys. Rev. **41**, 225 (1990).
[10] S. L. Cooper, D. Reznick, A. L. Kotz, M. A. Karlow, R. Liu, M. V. Klein, W. C. Lee, J. Giapintzakis, D. M. Ginzberg, B. W. Veal, and A. P. Paulikas, Phys. Rev. B **47**, 8233 (1993).
[11] B. S. Shastry and B. Shraiman, Int. J. Mod. Phys. B **5**, 365 (1991).
[12] A. Singh, Phys. Rev. B **48**, 6668 (1993).
[13] P. Sen and A. Singh, Phys. Rev. B **48**, 15792 (1993).
[14] A. Singh, Phys. Rev. B **43**, 3617 (1991).
[15] A. Singh and Z. Tešanović, Phys. Rev. B **41**, 614 (1990); **41**, 11457 (1990).
[16] J. Solyom, Z. Phys. **243**, 382 (1971).
[17] A. B. Harris, D. Kumar, B. I. Halperin, and P. C. Hohenberg, Phys. Rev. B **3**, 961 (1971).
[18] S. Tyc and B. I. Halperin, Phys. Rev. B **42**, 2096 (1990).
[19] P. Kopietz, Phys. Rev. B **41**, 9228 (1990).
[20] F. Nori, R. Merlin, S. Haas, A. W. Sandvik, and E. Dagotto, Phys. Rev. Lett. **75**, 553 (1995).
[21] M. J. Massey, R. Merlin, and S. M. Girvin, Phys. Rev. Lett. **69**, 2299 (1992).
[22] P. Knoll *et al.*, Phys. Rev. B **42**, 4842 (1990).
[23] A. V. Chubokov and D. M. Frenkel, Phys. Rev. Lett. **74**, 3057 (1995); Phys. Rev. B **52**, 9760 (1995).